iScience

CellPress
OPEN ACCESS

Article

The molecular signature of *BCR::ABL*^{P210} and *BCR::ABL*^{T315I} in a *Drosophila melanogaster* chronic myeloid leukemia model

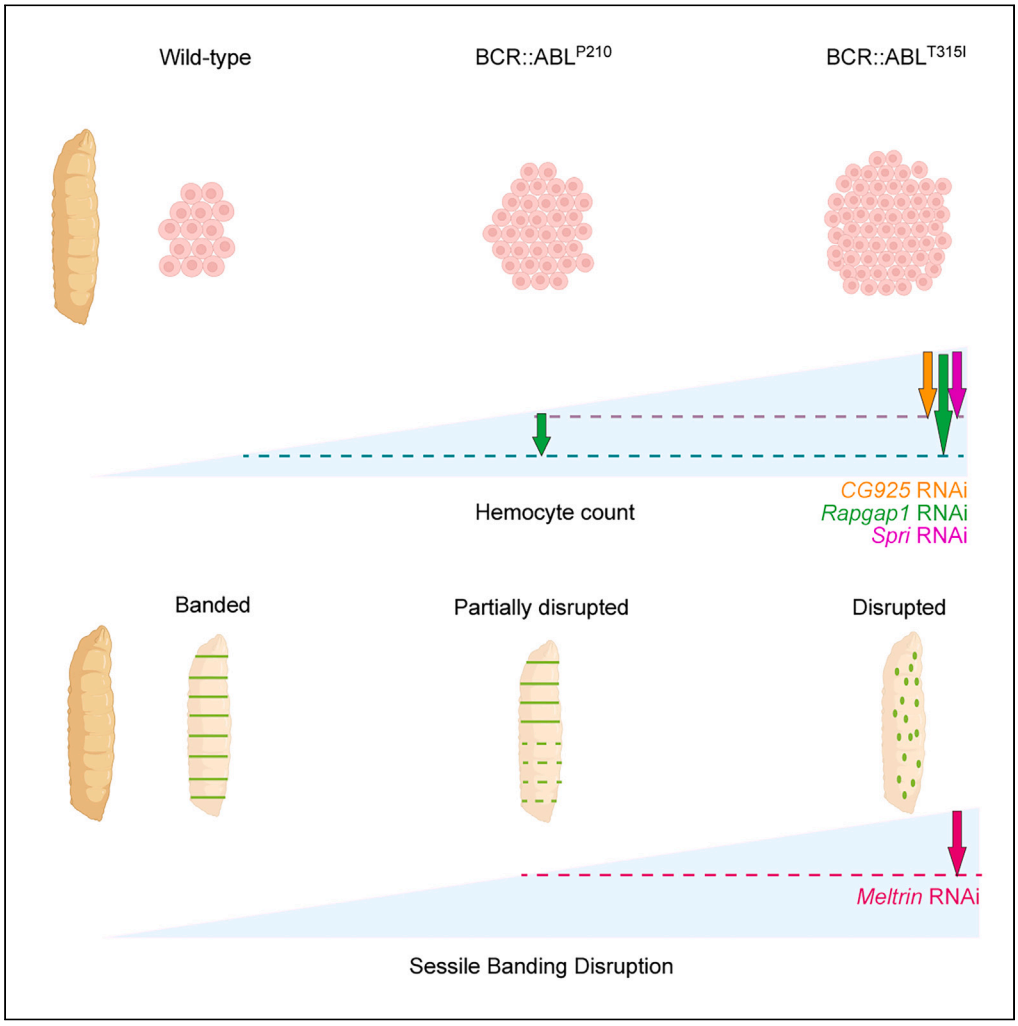

Amro Baassiri, Ali Ghais, Abdallah Kurdi, Elias Rahal, Rihab Nasr, Margret Shirinian

rn03@aub.edu.lb (R.N.)
ms241@aub.edu.lb (M.S.)

Highlights

BCR::ABL^{P210} and *BCR::ABL*^{T315I} exhibit unique molecular profiles explaining their severity

Dysregulated genes in *Drosophila* CML models may serve as promising therapeutic targets

Knockdown of key deregulated genes rescues hemocyte phenotypes in the *Drosophila* CML model

Baassiri et al., iScience *27*, 109538
April 19, 2024
https://doi.org/10.1016/j.isci.2024.109538

iScience

CellPress
OPEN ACCESS

Article

The molecular signature of *BCR::ABL*^{P210} and *BCR::ABL*^{T315I} in a *Drosophila melanogaster* chronic myeloid leukemia model

Amro Baassiri,[1] Ali Ghais,[2] Abdallah Kurdi,[3] Elias Rahal,[2,4] Rihab Nasr,[1,5,*] and Margret Shirinian[2,4,6,5,*]

SUMMARY

Chronic myeloid leukemia (CML) is a clonal hematopoietic stem cell disorder resulting from a balanced translocation leading to *BCR::ABL1* oncogene with increased tyrosine kinase activity. Despite the advancements in the development of tyrosine kinase inhibitors (TKIs), the T315I gatekeeper point mutation in the BCR::ABL1 gene remains a challenge. We have previously reported in a *Drosophila* CML model an increased hemocyte count and disruption in sessile hemocyte patterns upon expression of *BCR::ABL1*^{p210} and *BCR::ABL1*^{T315I} in the hemolymph. In this study, we performed RNA sequencing to determine if there is a distinct gene expression that distinguishes *BCR::ABL1*^{p210} and *BCR::ABL1*^{T315I}. We identified six genes that were consistently upregulated in the fly CML model and validated in adult and pediatric CML patients and in a mouse cell line expressing *BCR::ABL1*^{T315I}. This study provides a comprehensive analysis of gene signatures in *BCR::ABL1*^{p210} and *BCR::ABL1*^{T315I}, laying the groundwork for targeted investigations into the role of these genes in CML pathogenesis.

INTRODUCTION

The hallmark of chronic myeloid leukemia (CML), a clonal hematopoietic stem cell disorder, is the Philadelphia chromosome which results from a balanced translocation between chromosomes 9 and 22.[1] It creates the *BCR::ABL1* oncogene that encodes for the BCR::ABL1 fusion protein which demonstrates an increased tyrosine kinase activity.[2] The development of tyrosine kinase inhibitors (TKIs) has changed the natural course of this disease. Nowadays, patients with CML who respond well to treatment have a relatively normal life expectancy.[3,4] However, the notorious T315I (*BCR::ABL*^{T315I}) gatekeeper point mutation remains elusive to a great extent since it is completely resistant to first and second generation TKIs.[5,6] Currently, the only available drugs that patients with *BCR::ABL*^{T315I} respond to are the third generation TKI and the allosteric inhibitor ponatinib and asciminib, respectively.[7,8] However, ponatinib is associated with hepatotoxicity and serious cardiovascular events.[8–10] Some frequent adverse events reported with asciminib include myelosuppression, thrombocytopenia, leukopenia, and hemorrhage.[7] Despite demonstrating a promising efficacy in chronic-phase CML patients with *BCR::ABL*^{T315I}, both drugs have less than a 50% response rate in accelerated and blast-phase CML patients with *BCR::ABL*^{T315I}.[7,11,12] Therefore, there is a critical unmet clinical need to find novel potential targets against *BCR::ABL*^{T315I}.

We previously validated transgenic CML fly models expressing *BCR::ABL*^{P210} and *BCR::ABL*^{T315I} in the eye and hemolymph.[13,14] Upon expression in the eye, flies presented with rough eyes and architectural distortion in their ommatidia.[13] The expression in the hemolymph resulted in an increased hemocyte count along with a disruption in the sessile hemocytes' banding pattern.[14] Moreover, in both models, expression of the *BCR::ABL*^{T315I} demonstrated an exacerbated phenotype than that of *BCR::ABL*^{P210}.[13,14] The highly conserved hematopoietic system between humans and *Drosophila* associated with the observed phenotypic changes in our CML hematopoietic model demonstrates potential to identify novel targets against the wild-type *BCR::ABL*^{P210} and *BCR::ABL*^{T315I} mutant should we unravel the molecular signatures of our *BCR::ABL*^{P210} and *BCR::ABL*^{T315I} CML models, respectively.[15,16] In fact, several genes that play a role in blood cell development with a potential involvement in human leukemia have been studied via this model. *hopscotch* which encodes the *Drosophila* homologue of JAK kinase was identified to play a significant role in human leukemia via the JAK/STAT pathway.[17] As such, we extracted the hemolymph from our hematopoietic CML *Drosophila* models and unraveled their transcriptome. Furthermore, to validate our data, we cross-referenced them with the transcriptome of adult and pediatric patients with CML, and a mouse cell line harboring the *BCR::ABL*^{T315I} mutation. We then targeted the cross-referenced genes that were overexpressed when compared to control utilizing RNAi flies and assessed for total or partial

[1]Department of Anatomy, Cell Biology and Physiological Sciences, Faculty of Medicine, American University of Beirut, Beirut, Lebanon
[2]Department of Experimental Pathology and Immunology, Faculty of Medicine, American University of Beirut, Beirut, Lebanon
[3]Department of Biochemistry and Molecular Genetics, Faculty of Medicine, American University of Beirut, Beirut, Lebanon
[4]Center for Infectious Diseases Research, American University of Beirut Medical Center, Beirut, Lebanon
[5]These authors contributed equally
[6]Lead contact
*Correspondence: rn03@aub.edu.lb (R.N.), ms241@aub.edu.lb (M.S.)
https://doi.org/10.1016/j.isci.2024.109538

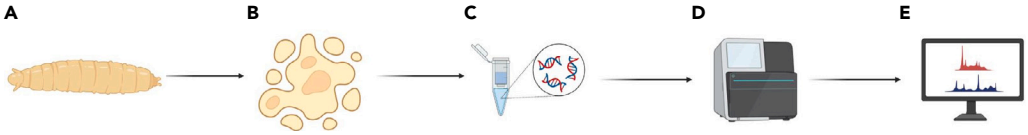
A
B
C
D
E

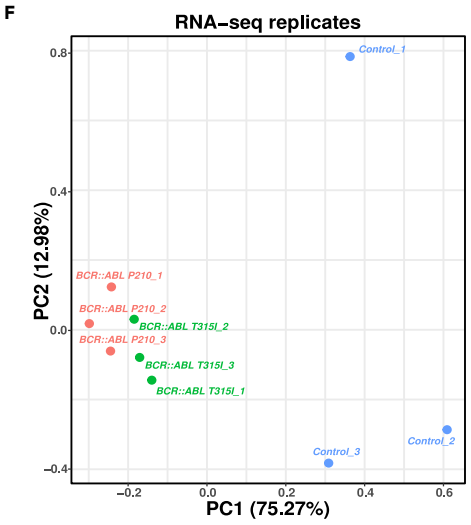
F
RNA−seq replicates
PC2 (12.98%)
PC1 (75.27%)
Control_1
Control_2
Control_3
BCR::ABL P210_1
BCR::ABL P210_2
BCR::ABL P210_3
BCR::ABL T315I_1
BCR::ABL T315I_2
BCR::ABL T315I_3

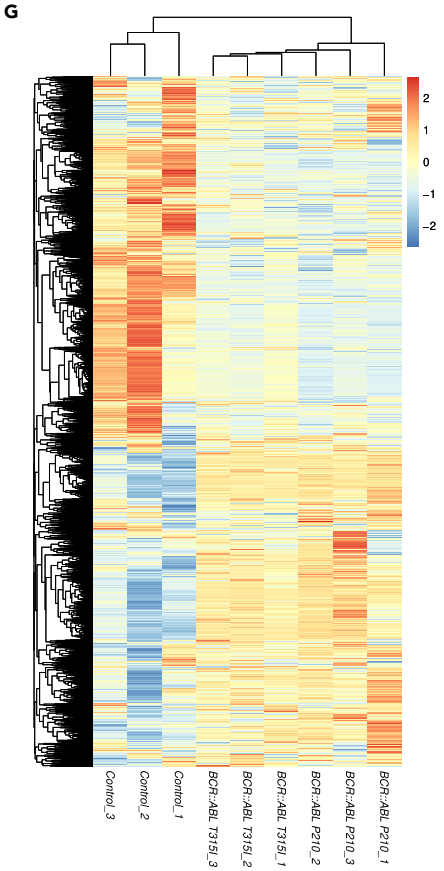
G
Control_3
Control_2
Control_1
BCR::ABL T315I_3
BCR::ABL T315I_2
BCR::ABL T315I_1
BCR::ABL P210_2
BCR::ABL P210_3
BCR::ABL P210_1

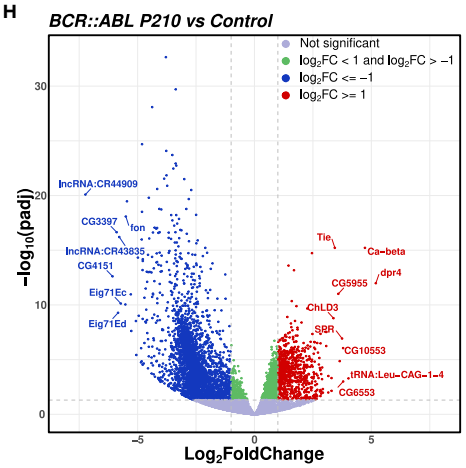
H
BCR::ABL P210 vs Control
Not significant
log2FC < 1 and log2FC > −1
log2FC <= −1
log2FC >= 1
−log10(padj)
Log2FoldChange
lncRNA:CR44909
CG3397
fon
lncRNA:CR43835
CG4151
Eig71Ec
Eig71Ed
Tie
Ca−beta
dpr4
CG5955
ChLD3
SPR
CG10553
tRNA:Leu−CAG−1−4
CG6553

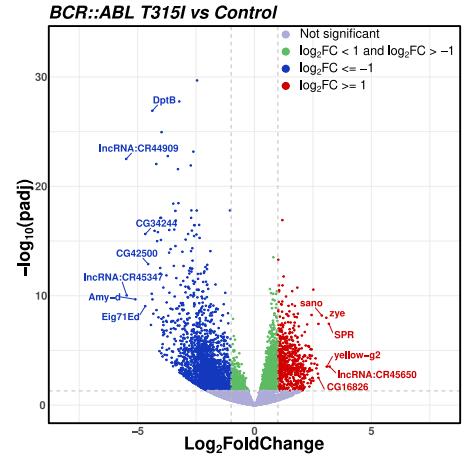
BCR::ABL T315I vs Control
Not significant
log2FC < 1 and log2FC > −1
log2FC <= −1
log2FC >= 1
−log10(padj)
Log2FoldChange
DptB
lncRNA:CR44909
CG34244
CG42500
lncRNA:CR45347
Amy−d
Eig71Ed
sano
zye
SPR
yellow−g2
lncRNA:CR45650
CG16826

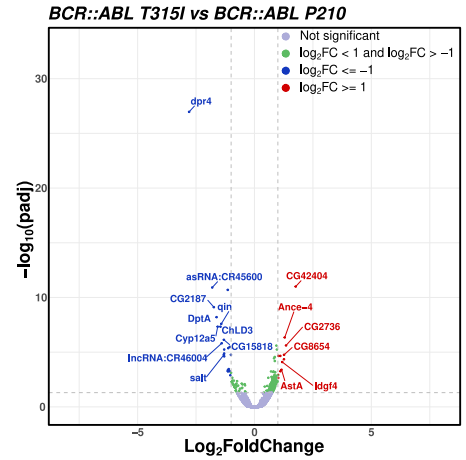
BCR::ABL T315I vs BCR::ABL P210
Not significant
log2FC < 1 and log2FC > −1
log2FC <= −1
log2FC >= 1
−log10(padj)
Log2FoldChange
dpr4
asRNA:CR45600
CG2187
qin
DptA
ChLD3
Cyp12a5
CG15818
lncRNA:CR46004
salr
CG42404
Ance−4
CG2736
CG8654
AstA
Idgf4

Figure 1. The molecular signatures of control, BCR::ABL^{P210}, and BCR::ABL^{T315I} hemolymph samples from *Drosophila melanogaster* models of chronic myeloid leukemia

(A) Third-instar larva were collected then (B) bled to collect their hemolymph.

(C) RNA extracted from hemocytes that (D) underwent RNA sequencing.

(E) Transcriptomic data were analyzed.

(F) Principal component analysis (PCA) of 9 distinct RNA-seq samples (3 samples from each genotype) highlighting the similarity between biological replicates of the same genotype and the difference between different genotypes. Markedly, the BCR::ABL^{P210} and BCR::ABL^{T315I} samples are relatively like each other compared to control.

(G) A hierarchical clustering of all genes in the samples based on similarity of their gene expression profiles (columns) and their corresponding gene specific expression values (rows). The heatmap generated displays similar gene profiles of BCR::ABL^{P210} and BCR::ABL^{T315I} samples and their differences compared to control. Red: relatively high expression; Blue: relatively low expression. The ratio values normalized by row.

(H) Volcano plots showing differentially expressed genes (DEGs) in each comparison between genotypes. Upregulated genes ($Log_2FC \geq 1$), downregulated genes ($Log_2FC \leq -1$), and genes with $-1 < Log_2FC > 1$ are represented by red, blue, and green dots, respectively. The gray dotted line represents the significant cutoff (p-adj value ≤ 0.05).

rescue of hemocyte count and/or sessile banding pattern in the attempt to find novel potential targets for the wild-type *BCR::ABL^{P210}* and *BCR::ABL^{T315I}* mutant.

RESULTS

BCR::ABL^{P210} and BCR::ABL^{T315I} share similar expression profiles but distinctly different from that of the control

We have previously shown that expression of *BCR::ABL^{P210}* and *BCR::ABL^{T315I}* result in detrimental eye phenotypes in adult *Drosophila* associated with an increase in hemocyte count, with a higher severity observed, for both phenotypes, in *BCR::ABL^{T315I}* flies.[14] To investigate if these phenotypic differences can be attributed to molecular changes, we collected hemocytes from flies expressing *BCR::ABL^{P210}* and *BCR::ABL^{T315I}*. Subsequently, we performed RNA extraction and sequencing to analyze the molecular profiles (Figures 1A–1E). The PCA plot provides a visual representation of the expression patterns in both *BCR::ABL^{P210}* and *BCR::ABL^{T315I}* samples within their respective groups, as well as the similarities between the two groups (Figure 1F). This observation is further supported by the heatmap analysis (Figure 1G), which clearly illustrates distinct molecular signatures for *BCR::ABL^{P210}* and *BCR::ABL^{T315I}* that are noticeably different from the control group. In the transcriptomic analysis, we observed that both *BCR::ABL^{P210}* and *BCR::ABL^{T315I}* exhibited differential gene expression compared to the control group. Specifically, when considering a p-adjusted value of less than 0.05 and an absolute Log2FC greater than 1, *BCR::ABL^{P210}* had a total of 3,651 differentially expressed genes (789 upregulated and 2,862 downregulated) compared to the control group. Similarly, *BCR::ABL^{T315I}* had a total of 3254 differentially expressed genes (622 upregulated and 2,632 downregulated) compared to the control group (Figure 1H). Notably, when comparing *BCR::ABL^{P210}* to *BCR::ABL^{T315I}*, only 35 genes were differentially expressed (12 upregulated and 23 downregulated) in *BCR::ABL^{T315I}*.

The top 10 downregulated genes in *BCR::ABL^{P210}* compared to control in descending order were *lncRNA:CR44909*, *CG4151*, *CG3397*, *Eig71Ed*, *lncRNA:CR43835*, *lncRNA:CR40469*, *Eig71Ec*, *CG17105*, *fon*, and *Idgf5*. Meanwhile the top 10 downregulated genes in *BCR::ABL^{T315I}* compared to control in descending order were *lncRNA:CR44909*, *lncRNA:CR45347*, *Amy-d*, *Eig71Ed*, *CG34244*, *CG42500*, *CG4367*, *CG17105*, *DptB*, and *CG13606*.

The top 10 upregulated genes in *BCR::ABL^{P210}* compared to control in descending order were *dpr4*, *Ca-beta*, *tRNA: Leu-CAG-1-4*, *CG6553*, *CG10553*, *SPR*, *BomS2*, *CG5955*, *Tie*, and *ChLD3*. Whereas the top 10 upregulated genes in *BCR::ABL^{T315I}* compared to control in descending order were *lncRNA:CR45650*, *SPR*, *yellow-g2*, *zye*, *sano*, *CG33462*, *CG16826*, *CG15370*, *CG3906*, and *CG16710*. The majority of the genes found to be dysregulated in our analysis lack annotation. However, among the identified dysregulated genes, we observed the presence of several long noncoding RNAs (lncRNAs) as well as genes encoding various enzymes, including oxidoreductases, amylases, and serine-type endopeptidases. Additionally, we identified genes involved in defense responses to bacteria, cell-matrix adhesion, and tyrosine kinases associated with cell survival and migration.

Expression of BCR::ABL^{P210} and BCR::ABL^{T315I} shows enrichment of the Toll/Imd signaling as well as other metabolic and developmental pathways

Pathway analysis showed that pathways related to cellular division as well as defense to bacterial infection, cell matrix and visceral muscle development are upregulated in *BCR::ABL^{P210}* compared to *control flies* (Figure 2A) whereas pathways related to carbohydrate catabolic processes and glucose metabolic pathways are downregulated (Figure 2B). Comparing *BCR::ABL^{T315I}* and *control* transcriptomes (Figures 2C and 2D) shows similar pathways enrichment as to *BCR::ABL^{P210}*. Meanwhile, pathway analysis comparing *BCR::ABL^{P210}* and *BCR::ABL^{T315I}* transcriptome showed two pathways that were enriched. Purine metabolism and humoral immune response related pathways (Figures 2E and 2F). Further analysis of deregulated genes in humoral immune pathways indicated the deregulation of genes involved in Toll/IMD pathways such as *Diptericin A*, *Diptericin B*, and *ADGF-D*, respectively. *Diptericin A* and *Diptericin B* were downregulated in *BCR::ABL^{T315I}* when compared to *BCR::ABL^{P210}* with Log2FC values of −1.62 and −1.1, respectively. *ADGF-D* was overexpressed in *BCR::ABL^{T315I}* when compared to *BCR::ABL^{P210}* with Log2FC value of 1.26. However, all three genes were downregulated in the *BCR::ABL^{P210}* and *BCR::ABL^{T315I}* flies when compared to control. The underexpression of these genes in *BCR::ABL^{P210}* and *BCR::ABL^{T315I}* flies, relative to the control, was validated by RT-qPCR ($p < 0.0001$) (Figures 4G–4I).

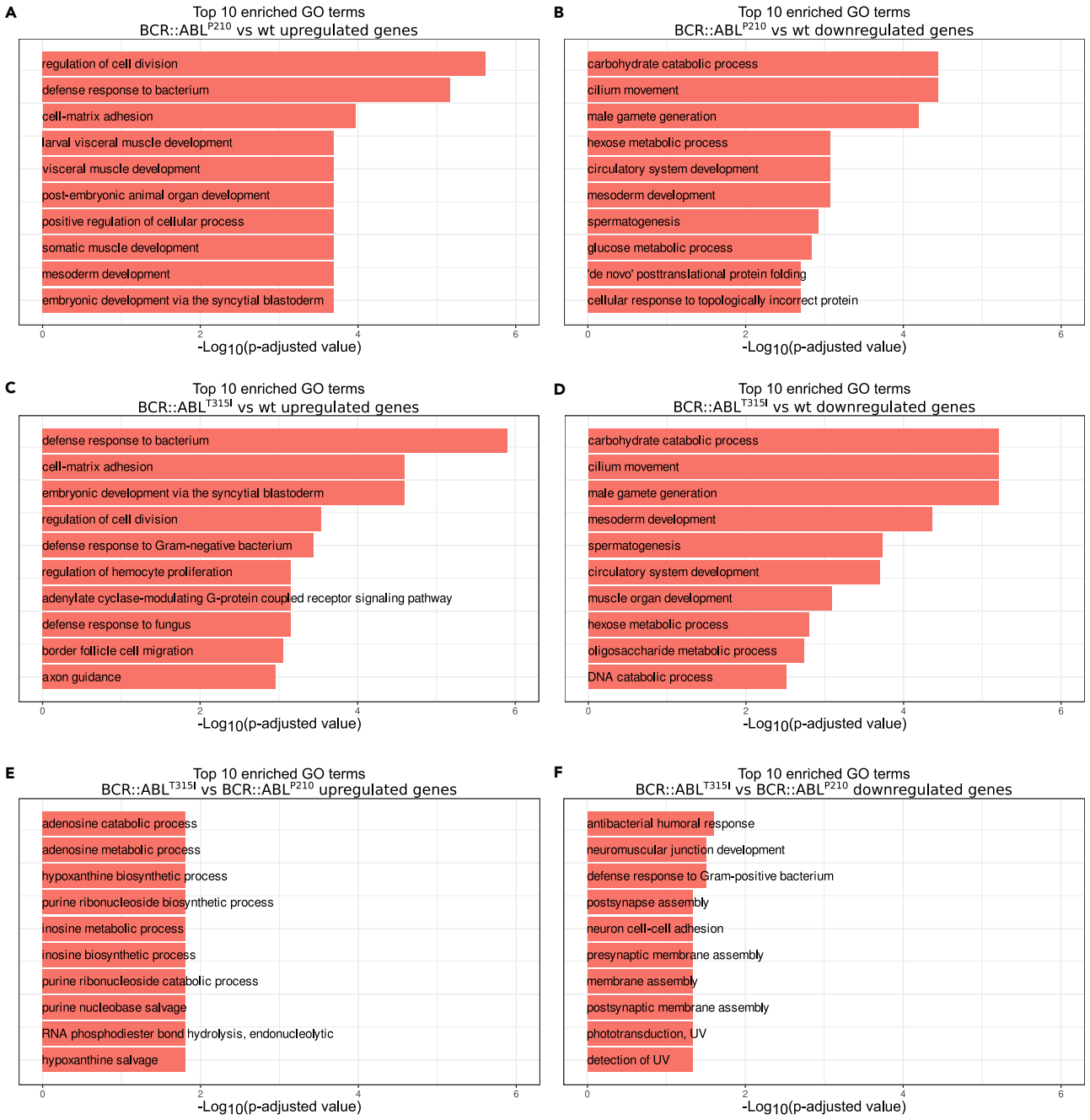

Figure 2. Gene ontology biological processes (GO-BP) enrichment analysis using FlyEnrichr: Enriched GO-BP terms in wild-type and mutant *BCR::ABL* compared to control in *Drosophila melanogaster* hemocytes

(A and B) corresponds to top 10 up and downregulated genes in *BCR::ABL^{P210}* compared to control.

(C and D) corresponds to top 10 up and downregulated genes in *BCR::ABL^{T315I}* compared to control.

(E and F) corresponds to top 10 up and downregulated genes in *BCR::ABL^{T315I}* compared to *BCR::ABL^{P210}*.

Identification of six potential common genes by integrating transcriptomic data from BCR::ABL ^{P210} and BCR::ABL ^{T315I} with samples from CML patients and a T315I BCR::ABL mouse cell line

We subsequently focused on the genes that exhibited common upregulation in both *BCR::ABL^{P210}* and *BCR::ABL^{T315I}*. We conducted two separate analyses: one comparing *BCR::ABL^{P210}* and *BCR::ABL^{T315I}* against adult and pediatric CML patient samples, and another comparing *BCR::ABL^{T315I}* against adult CML patient samples and *BCR::ABL^{T315I}* mouse cell line.[18–20] Through these analyses, we identified 16 common

A

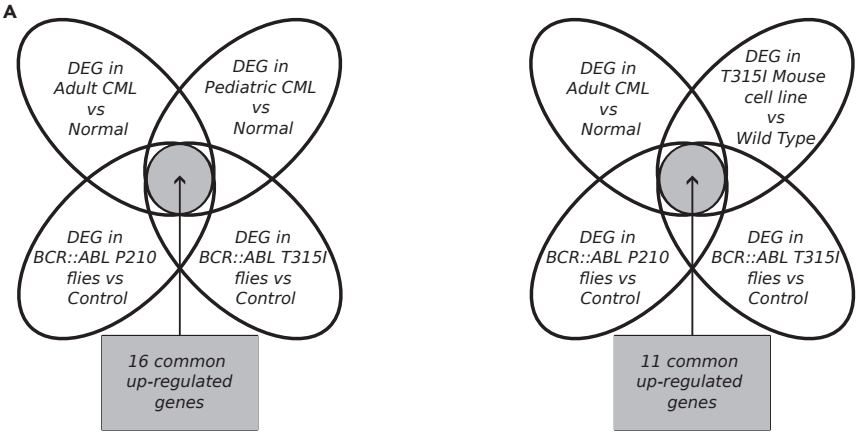

B

Fly gene	Human Orthologue	Function	Log_2(FC) fly BCR::ABL^{P210} vs Control	P-adjusted value	Log_2(FC) fly BCR::ABL^{T315I} vs Control	P-adjusted value	Log_2(FC) adult CML vs normal	P-adjusted value	Log_2(FC) T315I mouse cell line vs Control	P-adjusted value
Rapgap1	Rap1GAP	A GTPase activing protein (GAP); a major player in receptor-linked signaling pathways involved in cell growth and differentiation.[159]	2.154567272	0.0001009	1.976452157	0.0002	3.312886643	6.95E-05	0.976990485	0.0405220
Spri	RIN1	A Ras binding protein. Involved in multiple signal transduction pathways.[160]	1.245324254	8.17E-06	1.14004763	9.91E-07	2.000986811	0.0114862	1.511362722	0.0080466
Wb	LAMA5	Encodes for laminin, a major constituent of the basement membrane. Involved in cell adhesion, migration, and differentiation.[161]	1.453791834	0.0010979	1.448088447	0.000489	1.780538463	0.0011433	1.768025206	1.44E-08
Meltrin	ADAM8	A disintegrin and metalloproteinase. involved in cell-cell and cell-matrix interactions[162]	1.84263429	4.47E-05	1.710346948	8.03E-05	1.35811921	0.0231167	3.749742363	6.17E-12
CG9265	DHRS3	A short chain hydrogenase/reductase. Oxidizes and reduces a variety of substrates.[163]	1.07348834	0.0049110	1.10690467	0.003249	1.319264384	0.0231406	2.041389272	0.0038596
ZASP52	PDLIM5	A PDZ-LIM family member. A scaffold protein. Regulates cell structure and gene transcription.[164]	1.78623536	2.33E-05	1.706767887	1.43E-07	1.039877362	0.0216591	1.436912333	0.0003417

Figure 3. Cross-referencing *Drosophila* hemocyte transcriptomic data to CML patients and *T315 BCR::ABL mouse cell line* to validate and identify relevant targets

(A) 16 upregulated genes common to adult and pediatric patients with CML, while 11 upregulated genes common to adult patients with CML and *BCR::ABL*^{T315I} mouse cell line were identified.

(B) 6 potential upregulated targets namely, *Rapgap1*, *CG9265*, *meltrin*, *spri*, *wb*, and *zasp52* were identified.

upregulated genes in the first comparison and 11 common upregulated genes in the second comparison (Figure 3A). The purpose of the first analysis was to identify potential targets against the wild-type CML, while the second analysis aimed to identify potential targets against the T315I mutant type. Among these commonly upregulated genes, only six genes met our criteria: *Rapgap1*, *CG9265*, *meltrin*, *sprint (spri)*, *wing blister (wb)*, *and zasp52* (Figure 3B). These genes were selected based on our literature review and the availability of RNAi flies. Furthermore, we validated the overexpression of *rapgap1* ($p = 0.0008$ and $p = 0.0023$), *meltrin* ($p < 0.0001$), *spri* ($p = 0.0002$ and $p < 0.0001$), CG9265 ($p < 0.0001$ and $p = 0.0048$), and *zasp52* ($p < 0.0001$) in *BCR::ABL*^{P210} and *BCR::ABL*^{T315I}, respectively, compared to control flies (Figures 4 and 5A–5D, and 5F). Additionally, upon knocking down these genes in *BCR::ABL*^{P210} and *BCR::ABL*^{T315I,} we observed a significant decrease in gene expression of *rapgap1* ($p = 0.0058$ and $p = 0.0036$), *meltrin* ($p = 0.0066$), *spri* ($p = 0.0256$ and $p = 0.0029$), and CG9265 ($p = 0.0027$ and $p = 0.0222$) (Figures 4A–4D).

Partial rescue effects of downregulation of Rapgap1, spri, CG9265, and meltrin on hemocyte count and sessile banding pattern

To investigate if the downregulation of the selected upregulated genes could rescue the hemocyte count and/or sessile banding pattern phenotypes, RNAi flies targeting these genes were crossed with the *BCR::ABL*^{P210} and *BCR::ABL*^{T315I} screening lines. Knocking down *Rapgap1* resulted in a partial rescue of both *BCR::ABL*^{P210} ($p < 0.0001$) and *BCR::ABL*^{T315I} flies ($p < 0.0001$), reducing their hemocyte counts from an average of 1.16×10^6 cells to 7.61×10^5 and 1.94×10^6 cells to 6.52×10^5, respectively. Knocking down *Spri* and *CG9265* partially rescued *BCR::ABL*^{T315I} flies by decreasing their hemocyte counts to levels similar to *BCR::ABL*^{P210} ($p < 0.0001$), from an average of 1.94×10^6 cells to 1.22×10^6. However, knocking down *Spri* increased the hemocyte count in *BCR::ABL*^{P210} flies ($p = 0.0019$), from an average of 1.16×10^6 cells to 1.39×10^6. Additionally, knocking down *meltrin* and *wb* increased the hemocyte

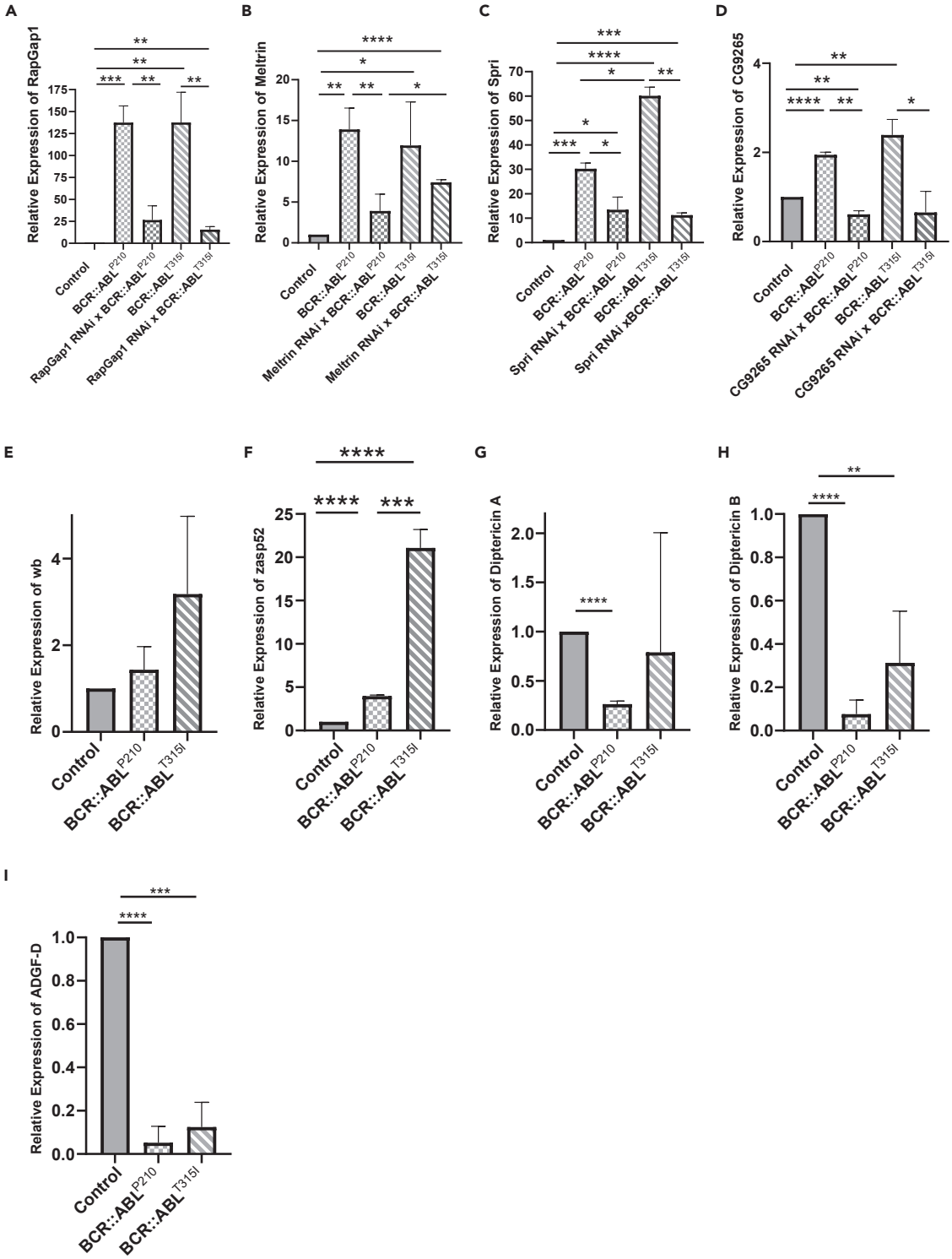

Figure 4. RT-qPCR validation of *Drosophila* hemocyte transcriptomic data and RNAi knockdown

(A–D and F) *Rapgap 1*, *meltrin*, *spri*, *CG9265*, and *zasp52* are overexpressed in *BCR::ABL*^{P210} and *BCR::ABL*^{T315I} larva when compared to the *wt* control. (E) *wb* expression in *BCR::ABL*^{P210} and *BCR::ABL*^{T315I} larvae where gene expression levels were not significant compared to the control. (G–I) *Diptericin A*, *Diptericin B*, and *ADGF-D* are underexpressed in *BCR::ABL*^{P210} and *BCR::ABL*^{T315I} larva when compared to *wt* control. (A–D) *meltrin*, *rapgap1*, *spri*, *and CG9265* respective RNAis when crossed with *BCR::ABL*^{P210} are underexpressed compared to *BCR::ABL*^{P210}. (A, C, and D) Rapgap 1, spri, and CG9265 respective RNAis when crossed with *BCR::ABL*^{T315I} are underexpressed. All genes were normalized to *RP49*. Error bars represent standard deviation. p -values (*, $p < 0.05$; **, $p < 0.01$; ***, $p < 0.001$; ****, $p < 0.0001$).

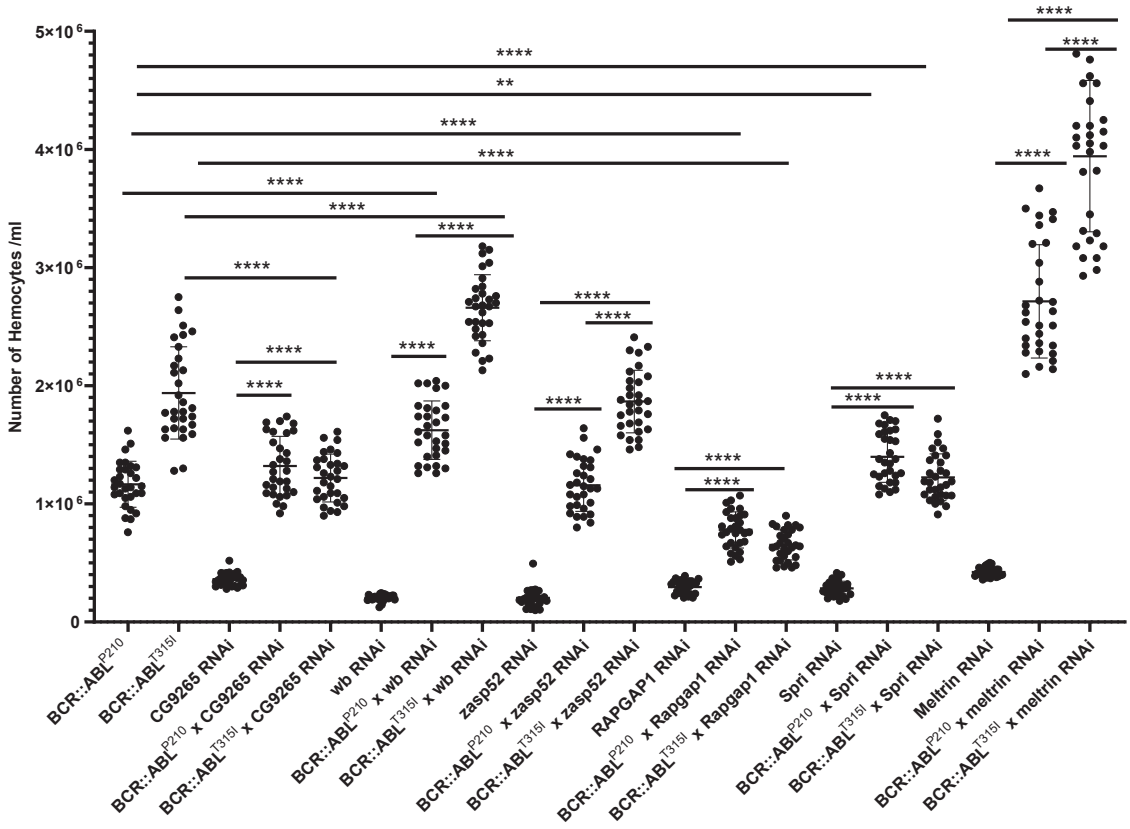

Figure 5. Enumeration of hemocytes in 3rd instar larva of *BCR::ABL^{P210}* and *BCR::ABL^{T315I}* alone and in combination with candidate gene knockdown

Rapgap1 RNAi partially rescued *BCR::ABL^{P210}* and *BCR::ABL^{T315I}* flies while *Spri* RNAi and *CG9265* RNAi partially rescued *BCR::ABL^{T315I}*. *Spri* RNAi increased hemocyte count in *BCR::ABL^{P210}* whereas *Meltrin* RNAi and *wb* RNAi increased hemocyte count in *BCR::ABL^{P210}* and *BCR::ABL^{T315I}* flies. Error bars represent standard deviation. p -values: **, $p < 0.01$; ****, $p < 0.0001$. (n = 30 triplicates).

count in both *BCR::ABL^{P210}* ($p < 0.0001$) and *BCR::ABL^{T315I}* flies ($p < 0.0001$). Knocking down *meltrin* increased the hemocyte count in *BCR::ABL^{P210}* and *BCR::ABL^{T315I}* flies from an average of 1.16×10^6 cells to 2.71×10^6 and 1.94×10^6 cells to 3.94×10^6, respectively. Knocking down *wb* increased the hemocyte count in *BCR::ABL^{P210}* and *BCR::ABL^{T315I}* flies from an average of 1.16×10^6 cells to 1.58×10^6 and 1.94×10^6 cells to 2.69×10^6, respectively. Knocking down *Zasp52* had no effect on either genotype (Figure 5). Regarding the sessile banding pattern, only knockdown of *meltrin* had an effect, partially rescuing the banding pattern in both *BCR::ABL^{P210}* ($p = 0.0175$) and *BCR::ABL^{T315I}* flies ($p = 0.0195$). The ratio of partial banding pattern increased from 3/30 to 11/30 in *BCR::ABL^{P210}* flies and from 0/30 to 5/30 in *BCR::ABL^{T315I}* flies (Figures 6A and 6B). *BCR::ABL^{P210} and BCR::ABL^{T315I}* expression was validated in control and screening lines (Figure S1A–S1C′).

Expression of BCR::ABL^{P210} and BCR::ABL^{T315I} in hemocytes leads to upregulation of lamellocyte differentiation markers

We investigated whether the overexpression of *BCR::ABL^{P210}* and *BCR::ABL^{T315I}* in hemocytes would lead to any significant changes in the different hemocyte lineages compared to the control. To assess this, we examined the gene expression of established markers for lamellocytes, plasmatocytes, and crystal cells to identify any differentially expressed genes (DEGs) among the three groups. Specifically, for lamellocytes, we analyzed the expression of prophenoloxidase 3 (*PPO3*), *ItgaPS4*, *mys*, *rhea*, *cher*, *betaTub60D*, *alphaTub85E*, and *lncRNA:CR44316*. For crystal cells, we focused on *PPO2*, *lozenge* pebbled (Figure 7).[21] The generated heatmap reveals a significant increase in lamellocyte differentiation in *BCR::ABL^{P210}* and *BCR::ABL^{T315I}* flies compared to the control group. Notably, the elevated expression of *betaTub60D*, *alphaTub85E*, and *lncRNA:CR44316* suggests a potential transition from an immature LM1 population to a more mature LM2 population.[22] Interestingly, the upregulation of *ItgaPS4* and *mys*, which are the *Drosophila* counterparts of human *ITGA4* and *ITGB1*, respectively, mirrors the increased expression of these orthologs in therapy resistant CML CD34$^+$ cells. It has been demonstrated that the binding of integrin α4β1 to its receptor VCAM-1 can support the quiescence of these cells, contributing to their resistance.[23,24] In contrast, crystal cell differentiation markers exhibit a distinct pattern in *BCR::ABL^{P210}* and *BCR::ABL^{T315I}* flies compared to the control group. Specifically, there is a decrease in *PPO2* expression and an increase in *lozenge* and *pebbled* expression (Figure 7). This alteration suggests a potential shift in the crystal cell population from mature CC2 cells to immature or transient intermediate state

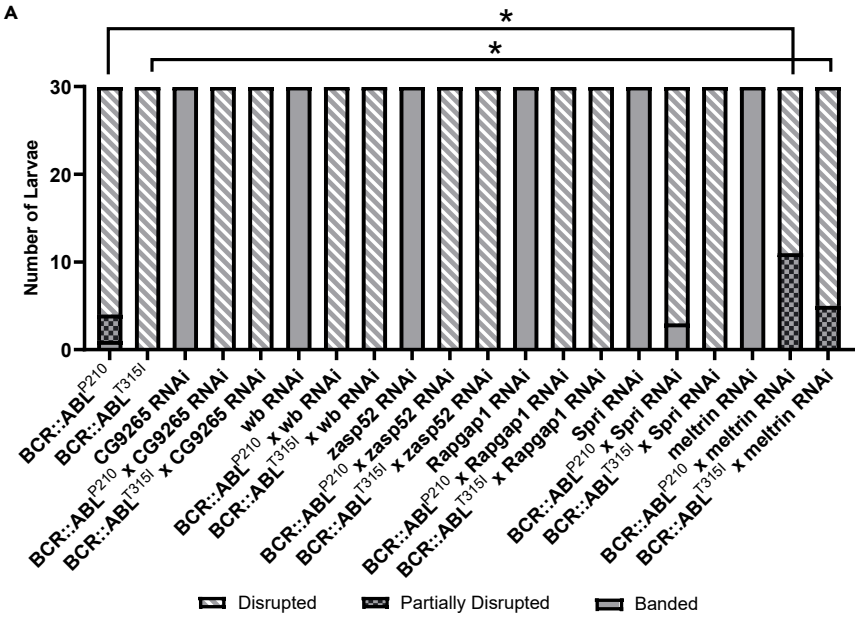
A
*
*
30
20
10
0
Number of Larvae
BCR::ABL^P210
BCR::ABL^T315I
CG9265 RNAi
BCR::ABL^P210 x CG9265 RNAi
BCR::ABL^T315I x CG9265 RNAi
wb RNAi
BCR::ABL^P210 x wb RNAi
BCR::ABL^T315I x wb RNAi
zasp52 RNAi
BCR::ABL^P210 x zasp52 RNAi
BCR::ABL^T315I x zasp52 RNAi
Rapgap1 RNAi
BCR::ABL^P210 x Rapgap1 RNAi
BCR::ABL^T315I x Rapgap1 RNAi
Spri RNAi
BCR::ABL^P210 x Spri RNAi
BCR::ABL^T315I x Spri RNAi
meltrin RNAi
BCR::ABL^P210 x meltrin RNAi
BCR::ABL^T315I x meltrin RNAi
Disrupted
Partially Disrupted
Banded

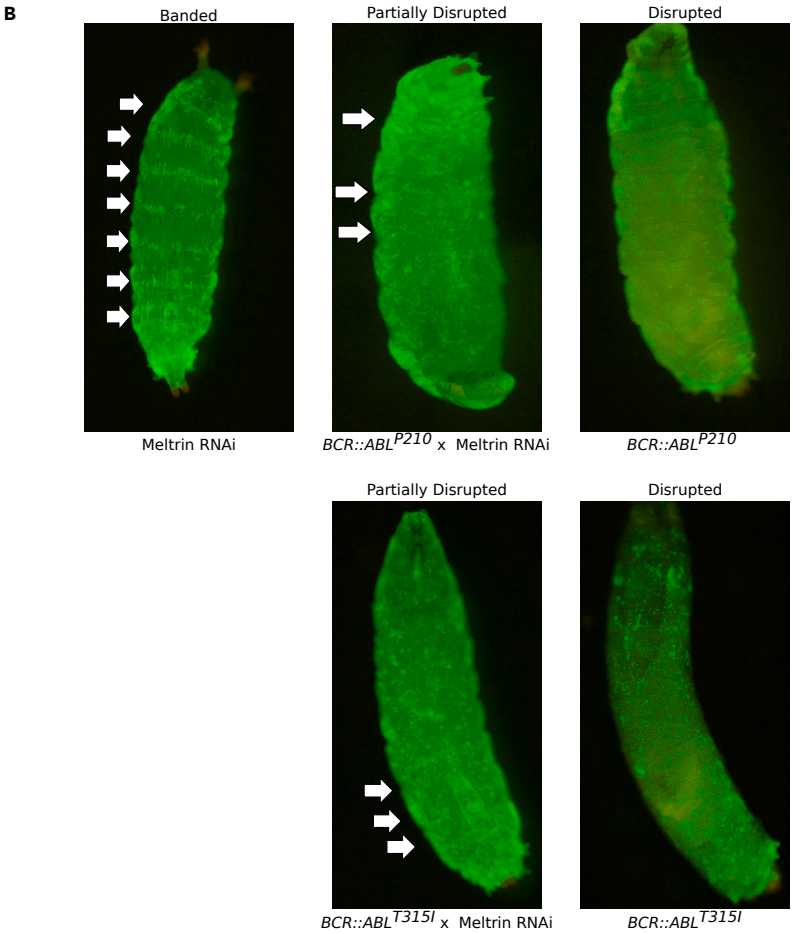
B
Banded
Partially Disrupted
Disrupted
Meltrin RNAi
BCR::ABL^P210 x Meltrin RNAi
BCR::ABL^P210
Partially Disrupted
Disrupted
BCR::ABL^T315I x Meltrin RNAi
BCR::ABL^T315I

Figure 6. Enumeration of banded, partially disrupted, and disrupted hemocyte sessile patterning in 3rd instar larva of *BCR::ABL*^{P210} and *BCR::ABL*^{T315I} alone and in combination with candidate gene knockdown larva

(A) *Meltrin* RNAi partially rescued banding in *BCR::ABL*^{P210} and *BCR::ABL*^{T315I} larva.

(B) *Meltrin* knockdown partially rescued banding patterns of *BCR::ABL*^{P210} and *BCR::ABL*^{T315I} larva from total disruption to partial disruption phenotype. p-value: *, $p < 0.05$. (n = 30 triplicates).

cells, known as CC1, which could represent another phenotype associated with CML in these flies.[22,25] Additionally, the plasmatocyte differentiation marker *NimC1* shows increased expression in both *BCR::ABL*^{P210} and *BCR::ABL*^{T315I} flies compared to the control group.

DISCUSSION

In this study, we demonstrate the use of a *Drosophila* model of CML to identify potential molecular targets by analyzing its transcriptome. To validate our findings, we compared the gene expression profiles with transcriptomic data from adult and pediatric CML patients, confirming the relevance of this model in studying leukemia and other human diseases. Among the top 10 downregulated genes in *BCR::ABL*^{P210} flies compared to wild-type controls, there were long non-coding genes and several uncategorized proteins. Among those genes is *CG3397* predicted to be involved in dehydro-D-arabinono-1,4-lactone biosynthetic process. Ecdysone-induced genes (*Eigs*) are involved in metamorphosis *(Eig71Ed)* and *(Eig71Ec)* in defense response to bacteria, respectively. Other genes such as *fondue* (*fon*) and *imaginal disc growth factor 5* (*Idgf5*), were associated with clotting reactions and the proliferation and motility of imaginal disk cells, respectively. In the *BCR::ABL*^{T315I} flies, the top 10 downregulated genes included long non-coding genes, five uncategorized proteins with unknown function and genes involved in defense response and the Imd pathway (*CG42500 Eig71Ed* and *Diptericin B*). It is worth noting that *lncRNA:cr44909*, *Eig71Ed*, and *CG17105* were common genes between *BCR::ABL*^{P210} and *BCR::ABL*^{T315I} in their top 10 under expressed genes compared to the wild-type control.[26]

The top 10 upregulated genes in *BCR::ABL*^{P210} flies compared to wild-type controls consist of three uncategorized proteins, one of which has an unknown function. *CG6553* is predicted to be active in the plasma membrane, while *CG5955* is predicted to be involved in threonine catabolic processes. The other genes have diverse functions, including synapse organization (*dpr4*), calcium ion transmembrane transport (*Ca-beta*), translation (*tRNA: Leu-CAG-1-4*), regulation of sleep behavior and reproductive behaviors (*SPR*), and chitin binding activity (*ChLD3*). Additionally, *Bomanin Short 2 (BomS2)* is a Toll signaling peptide, and *Tie*, a *tie-like receptor tyrosine kinase*, is upregulated. Tie is predicted to be a transmembrane tyrosine kinase receptor involved in cell survival and migration.

In the *BCR::ABL*^{T315I} flies compared to wild-type controls, the top 10 upregulated genes include five uncategorized proteins, three of which have unknown functions. *CG33462* and *CG16710* are predicted to enable serine-type endopeptidase activity. Additionally, there is a long non-coding gene with an unknown function. The remaining genes have various activities, including a female-specific role in egg development (*yellow-g2*), involvement as a structural component of chitin-based cuticle for cell-matrix adhesion (*zye*), and contribution to trachea development as a cytosolic protein (*sano*). *SPR* is the only gene common between *BCR::ABL*^{P210} and *BCR::ABL*^{T315I} in their top 10 overexpressed genes compared to wild-type controls.[26]

Regarding the identified potential targets, the knockdown of *Rapgap1* and *meltrin* showed partial rescue effects on the hemocyte count and sessile banding pattern, respectively, in both *BCR::ABL*^{P210} and *BCR::ABL*^{T315I} flies. Similarly, the knockdown of *CG9265* partially rescued the hemocyte count in *BCR::ABL*^{T315I} flies. However, it is worth noting that the knockdown of *meltrin* and *wb* had an oncogenic effect, leading to an increase in the hemocyte count in both *BCR::ABL*^{P210} and *BCR::ABL*^{T315I}.

Rapgap1 is a potential therapeutic target as its downregulation has been shown to partially rescue both the wild-type *BCR::ABL*^{P210} and *BCR::ABL*^{T315I} mutant. Rapgap1 is a GTPase-activating protein (GAP) that negatively regulates Rap1, which is involved in the ERK signaling pathway.[27] While Rapgap1 is typically considered a tumor suppressor and is often downregulated in cancers,[28] our CML *Drosophila* model showed its upregulation. Interestingly, studies have demonstrated that Rapgap1 can sometimes act as a tumor promoter. For example, it inhibits the coupling of adherens junctions to the actin cytoskeleton by inhibiting Rap1, leading to increased cell mobility and regulation of epithelial invagination in *Drosophila*.[29] Additionally, upregulation of *Rapgap1* has been shown to promote invasion in leukemic and squamous cell carcinoma cells through the secretion of metalloprotease MMP9.[30,31] These findings suggest that Rapgap1 may primarily influence tumor invasiveness rather than cell proliferation. Therefore, we can hypothesize that the reduction in hemocyte count observed upon Rapgap1 knockdown may be attributed to decreased cell mobility rather than a direct decrease in cell proliferation. However, we would expect the sessile banding pattern to have been restored or partially rescued, which was not the case. Another hypothesis could be that the depletion of Rapgap1 restored the expression of Rap1 which in turn could inhibit mTORC1 activation used by tumor cells as a means of regulating autophagy and prolonging their survival.[32–34] Therefore, we can consider monitoring phosphorylation status of mTORC1 substrates in the hemolymph of *BCR::ABL*^{P210} and *BCR::ABL*^{T315I} flies and comparing them to *Rapgap1* knockdown flies. A decrease in mTORC1 substrate phosphorylation would be supportive of this hypothesis. In a recent study that conducted a modifier screen for the rough eye phenotype in *BCR::ABL*^{P210}, it was demonstrated that expression of dominant negative Rab5, another family of RAS-like small GTP-binding protein, rescued the eye phenotypes induced by *BCR::ABL*^{P210}.[35] In our hemocyte system, we observed a slight downregulation of *Rab5* (Log2FC = 0.6). However, we observed a notable decrease in other Rab family members, including *Rab32* (log 2FC = −1.4), Rab3 (log 2FC = −2), and Rab26 (log 2FC = −2.45). These variations could be attributed to the tissue-specific expression patterns of these distinct Rab family proteins.

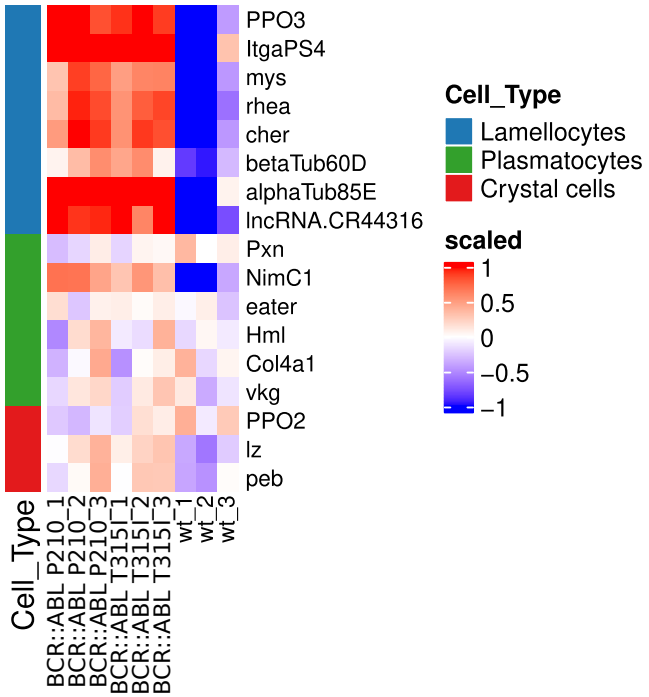

Figure 7. Gene expression levels of hemocyte differentiation markers in *BCR::ABL*^{P210} and *BCR::ABL*^{T315I} expressing 3rd instar larvae

The heatmap generated displays the differential gene expression of lamellocyte (*prophenoloxidase 3* (*PPO3*), *ItgaPS4*, *mys*, *rhea*, cher *betaTub60D*, *alphaTub85E*, and *lncRNA:CR44316*), plasmatocyte (*Pxn*, *NimC1*, *eater*, *hemolectin*, *col4a1*, and *viking*), and crystal cell (*PPO2*, *lozenge*, and *pebbled*) differentiation markers in control, *BCR::ABL*^{P210} and *BCR::ABL*^{T315I} flies. Red: relatively high expression; Blue: relatively low expression.

Regarding *CG9265*, it is an uncharacterized protein predicted to enable NAD-retinol dehydrogenase activity.[36] Its human counterpart, DHRS3, belongs to the short-chain dehydrogenases/reductases involved in the oxidation of steroids and retinol to retinaldehyde.[37] While retinoid therapy has demonstrated antitumor effects in various cancers, including acute promyelocytic leukemia.[38] DHRS3 amplification has been negatively associated with several cancers, such as triple-negative breast cancer and papillary thyroid carcinomas.[39–41] In our study, *CG9265* was found to be overexpressed and its knockdown partially rescued the *BCR::ABL*^{T315I} flies but had no effect on the *BCR::ABL*^{P210} flies. Although we currently lack a clear explanation for these findings, the observed partial rescue suggests that *CG9265* plays a role and represents a potential target that requires further investigation. More studies are needed to elucidate its mechanism of action and its involvement in the pathway specific to *BCR::ABL*^{T315I}, as the knockdown *CG9265* only affected the T315I mutant and not the wild-type *BCR::ABL*^{P210}.

Meltrin, an extracellular matrix degrading proteinase, is the human ortholog of ADAM8, which belongs to the ADAM family known for its involvement in tumors through the regulation of integrin function and growth factor activities.[42] ADAM8, specifically, has been implicated in promoting invasiveness and migration in various cancers.[43] Interestingly, ADAM8 has been identified as a key player in TKI-resistant CML cells, and inhibiting its expression restores sensitivity to TKIs.[44] In line with these findings, we observed the upregulation of meltrin in both *BCR::ABL*^{P210} and *BCR::ABL*^{T315I} flies. Upon knockdown of *meltrin*, we observed a partial rescue of the sessile banding pattern in both genotypes, indicating a restoration of migratory ability. However, the knockdown of *meltrin* also resulted in an increase in the hemocyte count in both genotypes. This increase in hemocyte production may be a response to a stressful state. During embryonic development, meltrin is typically detected in neuroblasts, suggesting its involvement in nervous system development.[42] In *Drosophila*, defects in the neural system have been shown to trigger an immune response, leading to increased hemocyte production. For example, disruptions in the balance between odorant ligands and gamma-aminobutyric acid (GABA) levels can disturb the quiescence of medullary zone cells in the lymph gland, leading to their differentiation and an immune response.[45] Similarly, significant knockdown of meltrin, which may affect nervous system development, could induce a distress response in the fly, resulting in an immune reaction.

Wing blister (*wb*) encodes laminin α chains, an extracellular matrix component associated with the basement membrane that are involved in cell adhesion via their interaction with integrins. Its human ortholog LAMA5 is usually upregulated in cancers whereby it promotes angiogenesis, metastasis, and resistance to certain cancer treatments.[46,47] It was upregulated in *BCR::ABL*^{P210} and *BCR::ABL*^{T315I} flies when knocking down *Wing blister* (*wb*), we observed an increase in hemocyte count. Considering the broader context, wb involvement in cell adhesion suggests that the increase in hemocytes may be associated with the loss of the sessile banding pattern. It is possible that these hemocytes, which are supposed to be attached to the wall in the epidermal-muscular pockets, were affected by the RNAi-mediated disruption of laminin, leading to impaired cell adhesion rather than cell proliferation.

Spri, a guanine nucleotide exchange factor (GEF) and a Ras effector, is the human ortholog of RIN1.[48] It plays a regulatory role in *BCR::ABL1* and is highly associated with it. Overexpression of *RIN1* potentiates the expression of *BCR::ABL1*, while silencing it has been shown to increase sensitivity to tyrosine kinase inhibitors (TKIs).[49,50] The strong association of spri/RIN1 with *BCR::ABL1* explains the partial rescue of hemocyte count observed in BCR- $BCR::ABL^{T315I}$ flies upon *spri* knockdown. However, we could not explain the increase in hemocyte count observed in $BCR::ABL^{P210}$ flies. The increased severity of the phenotype in $BCR::ABL^{T315I}$ mutant flies compared to their wild-type counterpart $BCR::ABL^{P210}$ flies may be attributed to the higher expression of *spri* in the former than in the latter. Afar et al.[49] have demonstrated that RIN1, the human ortholog of *spri*, accelerates the growth rate of BCR::ABL1 cells both *in vitro* and *in vivo*, leading to growth factor independence. Additionally, they have shown that overexpression of *RIN1* restores the transformative potential of BCR::ABL1 cells with point mutations that may otherwise reduce their transformative capacity.[50] Moreover, Thai et al. have reported that overexpression of *RIN1* enhances BCR::ABL1 activity, as evidenced by increased tyrosine phosphorylation levels of CRKL, an SH2/SH3 adapter protein. Furthermore, they have established the reliance of the $BCR::ABL^{T315I}$ transformative process on RIN1.[50] These findings align with our observations from *spri* RNAi experiments, where we noted a partial rescue in hemocyte count in $BCR::ABL^{T315I}$ mutant flies, while the absence of even a partial rescue in the $BCR::ABL^{P210}$ flies underscores the specific role of this gene in the severity of $BCR::ABL^{T315I}$.

Lastly, zasp 52 is a scaffold protein involved in muscle attachment. Its human ortholog is PDLIM5.[51] In cancers, PDLIM5 is typically upregulated and contributes to cell differentiation and migration.[52] Similarly, we observed upregulation in $BCR::ABL^{P210}$ and $BCR::ABL^{T315I}$ flies; however, knocking *zasp 52* down did not result in any noticeable effect. In conclusion, our study provides valuable insights into the transcriptomic profile of our hematopoietic CML *Drosophila* models. The similarities in the molecular signatures of $BCR::ABL^{P210}$ and $BCR::ABL^{T315I}$ flies suggest common pathways involved in CML pathogenesis. We identified potential targets, including Rapgap1, CG9265, and Meltrin, which showed promising results in rescuing the observed phenotypes. Further studies are needed to elucidate the underlying mechanisms and pathways associated with these targets. Additionally, the identification of common targets of $BCR::ABL^{P210}$ and $BCR::ABL^{T315I}$ highlights their potential relevance in treating CML patients with and without the T315I mutation. Future research should focus on investigating the pathways associated with these targets to gain a better understanding of their role in leukemic phenotypes.

Limitations of the study

One limitation of this study is that it primarily focuses on the analysis of gene expression and phenotypic changes in a *Drosophila* CML model. While this model provides valuable insights into the underlying mechanisms, it may not fully capture the complexity and heterogeneity of human CML. Further studies using human cell lines or patient samples would be necessary to validate the findings and establish their clinical relevance. Additionally, the functional analysis of the identified genes was performed in flies, and their direct relevance to human CML and potential therapeutic targeting requires further investigation. Furthermore, whereas our literature review had produced numerous genes of interest, the availability of RNAi flies in stock limited our choice of targeted genes.

STAR★METHODS

Detailed methods are provided in the online version of this paper and include the following:

- KEY RESOURCES TABLE
- RESOURCE AVAILABILITY
  - Lead contact
  - Materials availability
  - Data and code availability
- EXPERIMENTAL MODEL AND STUDY PARTICIPANT DETAILS
  - Fly stocks
  - Crosses performed
- METHOD DETAILS
  - RNA extraction
  - Hemocyte bleed and count
  - Immunofluorescence
  - Larvae handling and imaging for sessile patterns
  - Quantitative reverse transcription polymerase chain reaction (qRT-PCR)
  - RNA sequencing and data analysis
- QUANTIFICATION AND STATISTICAL ANALYSIS
  - Statistical analysis

SUPPLEMENTAL INFORMATION

Supplemental information can be found online at https://doi.org/10.1016/j.isci.2024.109538.

ACKNOWLEDGMENTS

Stocks were obtained from the Bloomington Drosophila Stock Center (NIH P40OD018537) and Vienna Drosophila Resource Center (VDRC) were used in this study. We thank the *Drosophila*, the imaging and the genomic core facilities at the American University of Beirut. We also thank all group members of the Shirinian lab for critical reading and discussion of the paper. MS is supported by the Medical Practice Plan Fund at the American University of Beirut.

AUTHOR CONTRIBUTIONS

A.B. and A.G. performed the experiments in this study. A.B. led and performed the transcriptomic and functional studies and conducted data analysis and interpretation. A.G. performed RT-qPCR and performed data analysis. A.K. performed transcriptomic and GO analysis and contributed to the figure assembly of the manuscript. A.B., R.N., and M.S. designed the study. A.B., E.R., R.N., and M.S. were involved in data interpretation. A.B. wrote the manuscript. E.R., R.N., and M.S. reviewed and edited the manuscript. R.N. and M.S. supervised the study. M.S. funded the project. All authors have read and approved the final version.

DECLARATION OF INTERESTS

The authors declare no competing interests.

Received: October 27, 2023
Revised: February 1, 2024
Accepted: March 18, 2024
Published: March 18, 2024

REFERENCES

1. Cortes, J., Pavlovsky, C., and Saußele, S. (2021). Chronic myeloid leukaemia. Lancet *398*, 1914–1926.
2. Lugo, T.G., Pendergast, A.-M., Muller, A.J., and Witte, O.N. (1990). Tyrosine kinase activity and transformation potency of bcr-abl oncogene products. Science *247*, 1079–1082.
3. Sasaki, K., Strom, S.S., O'Brien, S., Jabbour, E., Ravandi, F., Konopleva, M., Borthakur, G., Pemmaraju, N., Daver, N., Jain, P., et al. (2015). Relative survival in patients with chronic-phase chronic myeloid leukaemia in the tyrosine-kinase inhibitor era: analysis of patient data from six prospective clinical trials. Lancet. Haematol. *2*, e186–e193.
4. Bower, H., Björkholm, M., Dickman, P.W., Höglund, M., Lambert, P.C., and Andersson, T.M.-L. (2016). Life expectancy of patients with chronic myeloid leukemia approaches the life expectancy of the general population. J. Clin. Oncol. *34*, 2851–2857.
5. Jabbour, E., Kantarjian, H., Jones, D., Breeden, M., Garcia-Manero, G., O'brien, S., Ravandi, F., Borthakur, G., and Cortes, J. (2008). Characteristics and outcomes of patients with chronic myeloid leukemia and T315I mutation following failure of imatinib mesylate therapy. Blood J. Am. Soc. Hematol. *112*, 53–55.
6. Nicolini, F.E., Hayette, S., Corm, S., Bachy, E., Bories, D., Tulliez, M., Guilhot, F., Legros, L., Maloisel, F., Kiladjian, J.-J., et al. (2007). Clinical outcome of 27 imatinib mesylate-resistant chronic myelogenous leukemia patients harboring a T315I BCR-ABL mutation. Haematologica *92*, 1238–1241.
7. Cortes, J.E., Hughes, T.P., Mauro, M.J., Hochhaus, A., Rea, D., Goh, Y.T., Janssen, J., Steegmann, J.L., Heinrich, M.C., Talpaz, M., et al. (2020). Asciminib, a first-in-class STAMP inhibitor, provides durable molecular response in patients (pts) with chronic myeloid leukemia (CML) harboring the T315I mutation: primary efficacy and safety results from a phase 1 trial. Blood *136*, 47–50.
8. Cortes, J.E., Kim, D.-W., Pinilla-Ibarz, J., le Coutre, P.D., Paquette, R., Chuah, C., Nicolini, F.E., Apperley, J.F., Khoury, H.J., Talpaz, M., et al. (2018). Ponatinib efficacy and safety in Philadelphia chromosome–positive leukemia: final 5-year results of the phase 2 PACE trial. Blood J. Am. Soc. Hematol. *132*, 393–404.
9. Luciano, L., Annunziata, M., Attolico, I., Di Raimondo, F., Maggi, A., Malato, A., Martino, B., Palmieri, F., Pane, F., Sgherza, N., and Specchia, G. (2020). The multi tyrosine kinase inhibitor ponatinib for chronic myeloid leukemia: Real-world data. Eur. J. Haematol. *105*, 3–15.
10. Casavecchia, G., Galderisi, M., Novo, G., Gravina, M., Santoro, C., Agricola, E., Capalbo, S., Zicchino, S., Cameli, M., De Gennaro, L., et al. (2020). Early diagnosis, clinical management, and follow-up of cardiovascular events with ponatinib. Heart Fail. Rev. *25*, 447–456.
11. Cortes, J.E., Kim, D.-W., Pinilla-Ibarz, J., Le Coutre, P., Paquette, R., Chuah, C., Nicolini, F.E., Apperley, J.F., Khoury, H.J., Talpaz, M., et al. (2013). A phase 2 trial of ponatinib in Philadelphia chromosome–positive leukemias. N. Engl. J. Med. *369*, 1783–1796.
12. Cortes, J.E., Kantarjian, H., Shah, N.P., Bixby, D., Mauro, M.J., Flinn, I., O'Hare, T., Hu, S., Narasimhan, N.I., Rivera, V.M., et al. (2012). Ponatinib in refractory Philadelphia chromosome–positive leukemias. N. Engl. J. Med. *367*, 2075–2088.
13. Outa, A.A., Abubaker, D., Bazarbachi, A., Sabban, M.E., Shirinian, M., and Nasr, R. (2020). Validation of a Drosophila model of wild-type and T315I mutated BCR-ABL1 in chronic myeloid leukemia: an effective platform for treatment screening. Haematologica *105*, 387–397.
14. Abubaker, D., Baassiri, A., Ghannam, M., Al Outa, A., Ghais, A., Rahal, E., Nasr, R., and Shirinian, M. (2022). Expression of chronic myeloid leukemia oncogenes BCR-ABL P210 and BCR-ABL T315I affect cellular and humoral innate immunity in Drosophila melanogaster. MicroPubl. Biol. *2022*.
15. Yu, S., Luo, F., and Jin, L.H. (2018). The Drosophila lymph gland is an ideal model for studying hematopoiesis. Dev. Comp. Immunol. *83*, 60–69.
16. Letourneau, M., Lapraz, F., Sharma, A., Vanzo, N., Waltzer, L., and Crozatier, M. (2016). Drosophila hematopoiesis under normal conditions and in response to immune stress. FEBS Lett. *590*, 4034–4051.
17. Amoyel, M., Anderson, A.M., and Bach, E.A. (2014). JAK/STAT pathway dysregulation in tumors: a Drosophila perspective (Elsevier), pp. 96–103.
18. Mu, C., Wu, X., Ma, H., Tao, W., Zhang, G., Xia, X., Shen, J., Mai, J., Sun, T., Sun, X., et al. (2016). Effective Concentration of a Multikinase Inhibitor within Bone Marrow Correlates with In Vitro Cell Killing in Therapy-Resistant Chronic Myeloid Leukemia. Mol. Cancer Ther. *15*, 899–910. https://doi.org/10.1158/1535-7163.MCT-15-0577-T.
19. Youn, M., Smith, S.M., Lee, A.G., Chae, H.-D., Spiteri, E., Erdmann, J., Galperin, I., Jones, L.M., Donato, M., Abidi, P., et al. (2021). Comparison of the transcriptomic signatures in pediatric and adult CML. Cancers *13*, 6263.
20. Huang, C.-Y., Chung, Y.-H., Wu, S.-Y., Wang, H.-Y., Lin, Z.-Y., Yang, T.-J., Feng, J.-M., Hu, C.-M., and Chang, Z.-F. (2022). Targeting Reductive Metabolic Shifts by T315I Mutation in BCR-ABL Myeloid Leukemia for Therapy. Preprint at bioRxiv. https://doi.org/10.1101/2022.03.22.485260.
21. Hultmark, D., and Andó, I. (2022). Hematopoietic plasticity mapped in Drosophila and other insects. Elife *11*, e78906.
22. Tattikota, S.G., Cho, B., Liu, Y., Hu, Y., Barrera, V., Steinbaugh, M.J., Yoon, S.-H., Comjean, A., Li, F., Dervis, F., et al. (2020). A single-cell survey of Drosophila blood. Elife *9*, e54818.
23. Chorzalska, A., Salloum, I., Shafqat, H., Khan, S., Marjon, P., Treaba, D., Schorl, C., Morgan, J., Bryke, C.R., Falanga, V., et al. (2014). Low

expression of Abelson interactor-1 is linked to acquired drug resistance in Bcr-Abl-induced leukemia. Leukemia *28*, 2165–2177.
24. Puissant, A., Dufies, M., Fenouille, N., Ben Sahra, I., Jacquel, A., Robert, G., Cluzeau, T., Deckert, M., Tichet, M., Chéli, Y., et al. (2012). Imatinib triggers mesenchymal-like conversion of CML cells associated with increased aggressiveness. J. Mol. Cell Biol. *4*, 207–220.
25. Koranteng, F., Cha, N., Shin, M., and Shim, J. (2020). The role of lozenge in Drosophila hematopoiesis. Mol. Cells *43*, 114–120.
26. Drysdale, R.; FlyBase Consortium (2008). FlyBase. In Drosophila. Methods in Molecular Biology, C. Dahmann, ed. (Humana Press), pp. 45–59. https://doi.org/10.1007/978-1-59745-583-1_3.
27. Chen, F., Barkett, M., Ram, K.T., Quintanilla, A., and Hariharan, I.K. (1997). Biological characterization of Drosophila Rapgap1, a GTPase activating protein for Rap1. Proc. Natl. Acad. Sci. USA *94*, 12485–12490.
28. Yang, Y., Zhang, J., Yan, Y., Cai, H., Li, M., Sun, K., Wang, J., Liu, X., Wang, J., and Duan, X. (2017). Low expression of Rap1GAP is associated with epithelial-mesenchymal transition (EMT) and poor prognosis in gastric cancer. Oncotarget *8*, 8057–8068.
29. Wang, Y.-C., Khan, Z., and Wieschaus, E.F. (2013). Distinct Rap1 activity states control the extent of epithelial invagination via α-catenin. Dev. Cell *25*, 299–309.
30. Qiu, T., Qi, X., Cen, J., and Chen, Z. (2012). Rap1GAP alters leukemia cell differentiation, apoptosis and invasion *in vitro*. Oncol. Rep. *28*, 622–628.
31. Mitra, R.S., Goto, M., Lee, J.S., Maldonado, D., Taylor, J.M.G., Pan, Q., Carey, T.E., Bradford, C.R., Prince, M.E., Cordell, K.G., et al. (2008). Rap1GAP promotes invasion via induction of matrix metalloproteinase 9 secretion, which is associated with poor survival in low N-stage squamous cell carcinoma. Cancer Res. *68*, 3959–3969.
32. Looi, C.-K., Hii, L.-W., Ngai, S.C., Leong, C.-O., and Mai, C.-W. (2020). The role of Ras-associated protein 1 (Rap1) in cancer: bad actor or good player? Biomedicines *8*, 334.
33. Mutvei, A.P., Nagiec, M.J., Hamann, J.C., Kim, S.G., Vincent, C.T., and Blenis, J. (2020). Rap1-GTPases control mTORC1 activity by coordinating lysosome organization with amino acid availability. Nat. Commun. *11*, 1416.
34. Goldsmith, J., Levine, B., and Debnath, J. (2014). Autophagy and cancer metabolism. Methods Enzymol. *542*, 25–57.
35. Lo Iacono, M., Signorino, E., Petiti, J., Pradotto, M., Calabrese, C., Panuzzo, C., Caciolli, F., Pergolizzi, B., De Gobbi, M., Rege-Cambrin, G., et al. (2021). Genetic Screening for Potential New Targets in Chronic Myeloid Leukemia Based on Drosophila Transgenic for Human BCR-ABL1. Cancers *13*, 293. https://doi.org/10.3390/cancers13020293.
36. Alliance of Genome Resources Consortium (2020). Alliance of Genome Resources Portal: unified model organism research platform. Nucleic Acids Res. *48*, D650–D658.
37. Adams, M.K., Belyaeva, O.V., Wu, L., and Kedishvili, N.Y. (2014). The retinaldehyde reductase activity of DHRS3 is reciprocally activated by retinol dehydrogenase 10 to control retinoid homeostasis. J. Biol. Chem. *289*, 14868–14880.
38. Altucci, L., Rossin, A., Raffelsberger, W., Reitmair, A., Chomienne, C., and Gronemeyer, H. (2001). Retinoic acid-induced apoptosis in leukemia cells is mediated by paracrine action of tumor-selective death ligand TRAIL. Nat. Med. *7*, 680–686.
39. Lou, S., Gao, H., Hong, H., Zhu, Z., and Zhao, H. (2021). Inhibition of retinoic acid receptor α phosphorylation represses the progression of triple-negative breast cancer via transactivating miR-3074-5p to target DHRS3. J. Exp. Clin. Cancer Res. *40*, 1–15.
40. Passon, N., Bregant, E., Sponziello, M., Dima, M., Rosignolo, F., Durante, C., Celano, M., Russo, D., Filetti, S., and Damante, G. (2015). Somatic amplifications and deletions in genome of papillary thyroid carcinomas. Endocrine *50*, 453–464.
41. Oler, G., Camacho, C.P., Hojaij, F.C., Michaluart, P., Jr., Riggins, G.J., and Cerutti, J.M. (2008). Gene expression profiling of papillary thyroid carcinoma identifies transcripts correlated with BRAF mutational status and lymph node metastasis. Clin. Cancer Res. *14*, 4735–4742.
42. Meyer, H., Von Ohlen, T., Panz, M., and Paululat, A. (2010). The disintegrin and metalloprotease Meltrin from Drosophila forms oligomers via its protein binding domain and is regulated by the homeobox protein VND during embryonic development. Insect Biochem. Mol. Biol. *40*, 814–823.
43. Mochizuki, S., and Okada, Y. (2007). ADAMs in cancer cell proliferation and progression. Cancer Sci. *98*, 621–628.
44. Miyauchi, M., Koya, J., Arai, S., Yamazaki, S., Honda, A., Kataoka, K., Yoshimi, A., Taoka, K., Kumano, K., and Kurokawa, M. (2018). ADAM8 is an antigen of tyrosine kinase inhibitor-resistant chronic myeloid leukemia cells identified by patient-derived induced pluripotent stem cells. Stem Cell Rep. *10*, 1115–1130.
45. Banerjee, U., Girard, J.R., Goins, L.M., and Spratford, C.M. (2019). Drosophila as a genetic model for hematopoiesis. Genetics *211*, 367–417.
46. Gordon-Weeks, A., Lim, S.Y., Yuzhalin, A., Lucotti, S., Vermeer, J.A.F., Jones, K., Chen, J., and Muschel, R.J. (2019). Tumour-derived laminin α5 (LAMA5) promotes colorectal liver metastasis growth, branching angiogenesis and notch pathway inhibition. Cancers *11*, 630.
47. Li, L., Li, Z., Lu, C., Li, J., Zhang, K., Lin, C., Tang, X., Liu, Z., Zhang, Y., Han, R., et al. (2022). Ibrutinib reverses IL-6-induced osimertinib resistance through inhibition of Laminin α5/FAK signaling. Commun. Biol. *5*, 155.
48. Szabó, K., Jékely, G., and Rørth, P. (2001). Cloning and expression of sprint, a Drosophila homologue of RIN1. Mech. Dev. *101*, 259–262.
49. Afar, D.E., Han, L., McLaughlin, J., Wong, S., Dhaka, A., Parmar, K., Rosenberg, N., Witte, O.N., and Colicelli, J. (1997). Regulation of the oncogenic activity of BCR-ABL by a tightly bound substrate protein RIN1. Immunity *6*, 773–782.
50. Thai, M., Ting, P.Y., McLaughlin, J., Cheng, D., Müschen, M., Witte, O.N., and Colicelli, J. (2011). ABL fusion oncogene transformation and inhibitor sensitivity are mediated by the cellular regulator RIN1. Leukemia *25*, 290–300.
51. Liao, K.A., González-Morales, N., and Schöck, F. (2016). Zasp52, a core Z-disc protein in Drosophila indirect flight muscles, interacts with α-actinin via an extended PDZ domain. PLoS Genet. *12*, e1006400.
52. Liu, X., Chen, L., Huang, H., Lv, J.-M., Chen, M., Qu, F.-J., Pan, X.-W., Li, L., Yin, L., Cui, X.-G., et al. (2017). High expression of PDLIM5 facilitates cell tumorigenesis and migration by maintaining AMPK activation in prostate cancer. Oncotarget *8*, 98117–98134.
53. Liao, Y., Smyth, G.K., and Shi, W. (2014). featureCounts: an efficient general-purpose read summarization program. Bioinformatics *30*, 923–930.
54. Love, M.I., Huber, W., and Anders, S. (2014). Moderated estimation of fold change and dispersion for RNA-seq data with DESeq2. Genome Biol. *15*, 550. https://doi.org/10.1186/s13059-014-0550-8.
55. Evans, C.J., Liu, T., and Banerjee, U. (2014). Drosophila hematopoiesis: markers and methods for molecular genetic analysis. Methods *68*, 242–251.
56. FastQC (2015.
57. Kim, D., Paggi, J.M., Park, C., Bennett, C., and Salzberg, S.L. (2019). Graph-based genome alignment and genotyping with HISAT2 and HISAT-genotype. Nat. Biotechnol. *37*, 907–915.
58. Danecek, P., Bonfield, J.K., Liddle, J., Marshall, J., Ohan, V., Pollard, M.O., Whitwham, A., Keane, T., McCarthy, S.A., Davies, R.M., and Li, H. (2021). Twelve years of SAMtools and BCFtools. GigaScience *10*, giab008.
59. Ulgen, E., Ozisik, O., and Sezerman, O.U. (2019). pathfindR: an R package for comprehensive identification of enriched pathways in omics data through active subnetworks. Front. Genet. *10*, 858.

STAR★METHODS

KEY RESOURCES TABLE

REAGENT or RESOURCE	SOURCE	IDENTIFIER
Antibodies		
Anti-Myc antibody (9E-10)	Gift from Bengt Hallberg	NA
Deposited data		
Bulk RNA-seq on hemocyte	GEO	GSE243439
Experimental models: Organisms/strains		
w^{1118}	BDSC	3605
IF/CyO; TM3sb/TM6tb	Gift from Zakaria Kambris	NA
UAS-BCR::ABL^{P210} (p210)	Al Outa et al.[13]	NA
UAS-BCR::ABL^{T315I} (T315I)	Al Outa et al.[13]	NA
Rapgap1-RNAi	VDRC	26721
Spri-RNAi 101164	VDRC	101164
CG9265-RNAi	VDRC	102456
Meltrin-RNAi	VDRC	3702
Wing blister (wb)-RNAi	VDRC	3141
Zasp52-RNAi	VDRC	102456
Hml Δ-Gal4/CyO; BCR::ABLp210 /TM6tb	This study	NA
Hml Δ-Gal4/CyO; BCR::ABLT315I /TM6tb	This study	NA
Oligonucleotides		
Diptericin A: 5′-ACGCCACGAGATTGGACTG-3′, 5′- CAGCTCGGTTCTGAGTTGC-3	This study	NA
Diptericin B, 5′-CTATTCATTGGACTGGCTTGTGC-3′, 5′- ATCGAATCCTTGCTTTGGGCT-3′	This study	NA
ADGF-D, 5′-GTGGTTTCTAGGTGCTTTGGT-3′, 5′- CTCCCTCAGTGTTTCATAGGGT-3′	This study	NA
Rapgap1, 5′-CTACGATGCGAGAGGAAATCC-3′, 5′-TCCTGTAGCACTTGGCCGTAT-3′	This study	NA
meltrin, 5′-TTCCATCAGTCGGAAGGAGAA-3′, 5′-CGGTCGTATCACAGTGTAAGTTG-3′	This study	NA
Spri, 5′-GTGCGTCATCTCGACCGTAT-3′, 5′-GGCTCCCCATTAAGCAGTGT-3′	This study	NA
wb, 5′-ATCGGATTGCGATAAGCGAAC-3′, 5′-CGCCGTGAGATTCCAGTGAC-3′	This study	NA
zasp52, 5′-GGCGTGAAGAGCATTGTCAA-3′, 5′-ATCGCTGTAAATGCCAACCG-3′	This study	NA

(*Continued on next page*)

Continued

REAGENT or RESOURCE	SOURCE	IDENTIFIER
CG9265, 5′-GTCAAGTCCTGTGGAATACCTG-3′, 5′-GGATAGCCGAAGGCAATGTAG-3′	This study	NA
Rp49, 5′-CGCTTCAAGGGACAGTATCTG-3′, 5′-AAACGCGGTTCTGCATGA-3′	This study	NA
Software and algorithms		
FastQC v 0.12.1	Andrews, S. (n.d.). FastQC A Quality Control tool for High Throughput Sequence Data.	http://www.bioinformatics.babraham.ac.uk/projects/fastqc/
HISAT2	Daehwan Kim et al.	https://github.com/DaehwanKimLab/hisat2
FeatureCounts	Liao, Y. et al.[53]	https://subread.sourceforge.net/
DESeq2	Love, M. et al.[54]	https://bioconductor.org/packages/deseq2/
R version 4.1.1	R Foundation	https://www.r-project.org

RESOURCE AVAILABILITY

Lead contact

Further information and requests for resources and reagents should be directed to and will be fulfilled by the lead contact, Margret Shirinian (ms241@aub.edu.lb).

Materials availability

This research did not produce novel reagents. All *Drosophila* lines utilized in this paper are accessible through stock centers or can be provided upon inquiry.

Data and code availability

- Bulk RNA-seq on hemocyte data have been deposited at GEO and is available under the accession number GSE243439.
- This paper does not report original code.
- Any additional information required to reanalyze the data reported in this paper is available from the lead contact upon request.

EXPERIMENTAL MODEL AND STUDY PARTICIPANT DETAILS

Fly stocks

Fly stocks used were w^{1118} (*wt*) (BDSC #3605), IF/CyO; TM3sb/TM6tb (gift from Dr. Zakaria Kambris), Hml Δ-Gal4; UAS-GFP (BDSC #30140), *UAS-BCR::ABL*^{P210} (p210) (FBtp0141454)[13] and *UAS-BCR::ABL*^{T315I} (T315I) (FBtp0141455).[13] RNAi flies were obtained from Vienna Drosophila Resource Center (VDRC): *Rapgap1*-RNAi (VDRC #26721), *Spri*-RNAi (VDRC # 101164), *CG9265*-RNAi (VDRC #102456), *meltrin*-RNAi (VDRC #3702), *wing blister* (*wb*)-RNAi (VDRC #3141), *Zasp52*-RNAi (VDRC #102456). The screening lines generated: Hml Δ-Gal4/CyO; *BCR::ABL*^{P210} /TM6tb and Hml Δ-Gal4/CyO; *BCR::ABL*^{T315I} /TM6tb. All crosses were performed at 29°C.

Crosses performed

Hml Δ-Gal4; UAS-GFP flies were crossed with W^{1118} (control), *UAS-BCR::ABL*^{P210}, and *UAS-BCR::ABL*^{T315I} for hemolymph collection, RNA extraction, RNA-sequencing, and qRT-PCR. Screening lines were crossed with RNAi flies whereby the selected progeny collected expressed green fluorescent protein (GFP) and were non-tubby (without TM6tb) since the genotype desired was either Hml Δ-Gal4/+; *BCR::ABL*^{P210} RNAi X or Hml Δ-Gal4/RNAi X; *BCR::ABL*^{P210} + (same case for *UAS-BCR::ABL*^{T315I}) depending on which chromosome the RNAi was. These underwent banding and hemocyte enumeration. Workflow is depicted in (Figures 1A–1E).

METHOD DETAILS

RNA extraction

For RNA-seq samples, 300 larvae were bled in 240-300 μl PBS then put in 700-760 μl of Trizol (TRI reagent, Sigma Aldrich). For the qRT-PCR, 150 larvae were bled in 120-160 μl PBS then put in 840-880 μl of Trizol, centrifuged at 12,000g for 15 mins at 4°C. For the validation of the RNAi system, 50 larvae were bled in 40-50 μl PBS then put in 950-960 μl of Trizol, centrifuged at 12,000g for 15 mins at 4°C. Then 200 μl of chloroform (Sigma-Aldrich) was added. Tubes were shaken well then centrifuged at 12,000g for 15 mins at 4°C. Upper layer was transferred to another

tube and added to it 0.1V 3M sodium acetate, 0.7V of isopropanol 100%, and 2 μl of glycoblue (Invitrogen), kept at room temperature for 10 mins, then centrifuged for 30 mins max speed at 4°C. Isopropanol was removed then RNA pellet was washed with 1 ml cold ethanol 70% (Sigma-Aldrich) which was centrifuged at max speed for 10 mins at 4°C. Ethanol was removed and the pellet was set to air dry for 10 mins under the hood. Pellet was resuspended in 20 μl Nuclease free water (Autoclaved milli-Q water) and then put on heat block at 55°C for 10 mins. The above was performed on three different biological replicates (N=3) with 300 third-instar larvae for each replicate for RNA-seq and 50-150 third-instar larvae for qRT-PCR.

Hemocyte bleed and count

Late wandering third-instar larvae were picked from the walls of the food vial with a pair of forceps and cleaned from food and debris by placing them in a 1X PBS containing petri plate before being transferred to a tissue paper to dry them. The larvae were placed in 10 μl of 1X-PBS that was placed on parafilm strip under a light microscope. Using two pairs of forceps the larval cuticle was pierced and hemolymph was released. The larva was left to bleed for 20 secs. The hemolymph bleed was pipetted and mixed with an equal volume of trypan blue. A total of 10 μl of the mix was placed in a Neubauer chamber (Buerker-Turk, Marienfeld, Germany) with a coverslip attached. The Neubauer chamber was placed under an Axiostar plus light microscope (Zeiss, Oberkochen, Germany) and number of cells in each of the four quadrants was noted down. Hemocyte number was then reported as hemocytes per milliliter of bleed. The average number of hemocytes was obtained from three different biological replicates (N=3) with ten third-instar larvae for each replicate. The total number of larvae used in each condition is (n=30).

Immunofluorescence

We performed hemocyte staining, to validate our screening lines. Late wandering third instar were bled in 10 μl of 1X-PBS in a 12 well plate using a modified protocol.[55] Then the bleed was transferred to slides and left to attach for 30 mins in a humidified chamber. The bleed was washed with 1X PBS- 0.3% Triton (PBST) twice for 5 mins and samples were then blocked in 5% Normal Goat Serum (NGS) in PBST (Dako, Santa Clara, CA) for 2 hours. Anti-Myc antibody (9E-10 kind gift from Bengt Hallberg) 1:300 was used on hemocytes overnight. Samples were washed with PBST 2x5 mins and incubated with secondary antibody Alexa-594 1:500 in 5%NGS PBST (Abcam, Cambridge, UK). Then, after 2 washes with PBST, Fluor shield Mounting Medium with DAPI (Abcam) was added and samples were then imaged using a laser scanning confocal microscope (Carl Zeiss Laser Scanning Microscopy 710, Jena, Germany).

Larvae handling and imaging for sessile patterns

Late wandering third-instar larvae were picked from the walls of the food vial with a pair of forceps and cleaned from food and debris by placing them in a petri plate containing 1X Phosphate Buffered Saline (PBS) (Sigma Aldrich, St. Louis, MO). After drying with tissue paper, the larvae were placed on a plate and kept at -20°C for 30-60 secs. The larvae were then imaged for sessile patterning using an SZX2-ILLT GFP Olympus microscope (Olympus, Tokyo, Japan) (modified protocol from Anderl et al. 2016). The above was performed on three different biological replicates (N=3) with ten third-instar larvae for each replicate. The total number of larvae used in each condition is (n=30).

Quantitative reverse transcription polymerase chain reaction (qRT-PCR)

Real time PCR was performed using SYBR green (Bio-Rad) and Bio-RAD CFX96 Real time system. The assessment was repeated for three biological replicates whereby each biological group included 50-150 third-instar larvae and each sample was run in triplicates. Relative gene expression was analyzed using the Livak and Schmittegn system (Livak and Schmittgen 2001) using the housekeeping gene *Ribosomal protein 49* (*Rp49*) as internal control. The Forward and Reverse primer (Macrogen, Seoul, South Korea) sequences were as follow: *Diptericin A,* 5′-ACGCCACGAGATTGGACTG-3′, 5′- CAGCTCGGTTCTGAGTTGC-3′; *Diptericin B,* 5′-CTATTCATTGGACTGGCTTGTGC-3′, 5′- ATCGA ATCCTTGCTTTGGGCT-3′; *ADGF-D,* 5′-GTGGTTTCTAGGTGCTTTGGT-3′, 5′- CTCCCTCAGTGTTTCATAGGGT-3′; *Rapgap1,* 5′-CTACGAT GCGAGAGGAAATCC-3′, 5′-TCCTGTAGCACTTGGCCGTAT-3′; *meltrin,* 5′-TTCCATCAGTCGGAAGGAGAA-3′, 5′-CGGTCGTATCACAGT GTAAGTTG-3′; *Spri,* 5′-GTGCGTCATCTCGACCGTAT-3′, 5′-GGCTCCCCATTAAGCAGTGT-3′; *wb,* 5′-ATCGGATTGCGATAAGCGAAC-3′, 5′-CGCCGTGAGATTCCAGTGAC-3′; *zasp52,* 5′-GGCGTGAAGAGCATTGTCAA-3′, 5′-ATCGCTGTAAATGCCAACCG-3′; *CG9265,* 5′-GT CAAGTCCTGTGGAATACCTG-3′ , 5′-GGATAGCCGAAGGCAATGTAG-3′; *Rp49,* 5′-CGCTTCAAGGGACAGTATCTG-3′, 5′-AAACGCGGTT CTGCATGA-3′.

RNA sequencing and data analysis

Utilizing the Illumina NovaSeq6000, we performed RNA sequencing with a 100bp paired end read and 40 million reads per sample. Raw fastq files were uploaded to Galaxy US server and were subjected to quality checks using FastQC.[56] Sequence alignment to dm6 reference genome was performed using HISAT2.[57] Alignment BAM files were sorted and indexed using SAMtools.[58] Raw read count over genomic features was done using featureCounts[53] and annotation GTF file from FlyBase release 6.45 with parameters (-t gene -g gene_symbol -s 2 -p -B). Differential expression analysis was performed using DESeq2[54] and genes with an absolute $\log_2$ fold change (Log_2FC) > 1 and a p-adjusted < 0.05 were considered differentially expressed. Gene ontology (GO) enrichment analysis of the differentially expressed genes was done using FlyEnrichr.[59] We cross-referenced the upregulated genes in *BCR::ABL*^{P210} and *BCR::ABL*^{T315I} against adult (10 patients) and pediatric (9 patients) CML patient samples (PRJNA687184) as well as *BCR::ABL*^{T315I} mouse cell line (PRJNA812502). The T315I-Bcr-Abl-32D cells were

generated via transduction of 32D cells with retrovirus carrying a T315I-mutant BCR-ABL (32Dp210T315I) gene[18] and subjected to transcriptomic analysis. Heatmap, volcano and bar plots, and principal component analysis (PCA) plots were generated using pheatmap, ggplot2, and ggfortify R packages, respectively.

QUANTIFICATION AND STATISTICAL ANALYSIS

Statistical analysis

Statistical analyses were performed using GraphPad Prism 6.0. RT-qPCR results were tested via an unpaired T-test. Hemocyte counts were compared through one-way ANOVA followed by Tukey's post-hoc test and banding patterns were tested via Chi-square test. P-values lower than 0.05 were considered statistically significant.